ISSN 1063-7850, Technical Physics Letters, 2016, Vol. 42, No. 11, pp. 1090–1093. © Pleiades Publishing, Ltd., 2016.
Original Russian Text © M.I. Vexler, G.G. Kareva, Yu.Yu. Illarionov, I.V. Grekhov, 2016, published in Pis'ma v Zhurnal Tekhnicheskoi Fiziki, 2016, Vol. 42, No. 21, pp. 62–69.

Resonant Electron Tunneling and Related Charging Phenomena in Metal–Oxide–p^+-Si Nanostructures

M. I. Vexler[a]*, G. G. Kareva[b], Yu. Yu. Illarionov[a, c], and I. V. Grekhov[a]
[a] *Ioffe Physical-Technical Institute, Russian Academy of Sciences, St. Petersburg, 194021 Russia*
[b] *Physical Faculty, St. Petersburg State University, St. Petersburg, 198504 Russia*
[c] *Institute for Microelectronics, TU Wien, Vienna, A-1040 Austria*
**e-mail: shulekin@mail.ioffe.ru*

Received April 29, 2016

Abstract—The j–V characteristics of the Al/thermal or electrochemical SiO$_2$(2–4 nm)/heavily doped p^+-Si nanostructures operating as a resonant-tunneling diode were measured and theoretically analyzed. The characteristics have specific features in the form of current steps and peaks, which are caused by electron transport between the silicon valence band and metal through discrete levels of the quantum well formed by the p^+-Si conduction band and SiO$_2$/p^+-Si interface. Resonant tunneling through the surface state levels and the appearance of a charge near this interface under certain conditions are discussed.

DOI: 10.1134/S1063785016110109

The physics of metal–thin oxide (e.g., SiO$_2$)–silicon structures has been studied fairly well. Many problems, including analysis of the electric charge and voltage distributions and calculation of tunnel currents, can be considered solved when the barrier parameters for a specific system are determined [1, 2]. However, the phenomenon of resonant tunneling (RT) in metal–insulator–semiconductor (MIS) structures even with the most frequently used combinations of materials, remains almost unexplored.

We demonstrated this interesting phenomenon in [3, 4]. The conditions for it were established upon depletion/inversion of an MIS nanostructure with a rather large band bending $q\varphi_s$ in p^+-Si: the RT occurs between the silicon valence (v) band and metal through levels E_i (i = 1, 2, ...) of the energy quantum well (QW, see right diagram in Fig. 1) [2]. One of the barriers is the p^+-Si band gap, and the other is the insulator. The semiconductor barrier in the samples studied in [3, 4] had a lower tunnel transparency T_s than the oxide ($T_s \ll T_{ox}$).

This Letter thoroughly analyzes the behavior of RT diodes (RTDs) based on the MIS structure and interprets the observed peculiarities. For this purpose, we assumed that discrete levels E_n involved in the RT can be not only the QW levels, but also levels E_{ti} of different origin, which are associated with the surface states (SS) at the Si–insulator interface [5]. Each of levels E_n (energy reference is E_{c0}) is involved in the RT under the condition $q\varphi_s - E_g > E_n$. The tunneling direction is

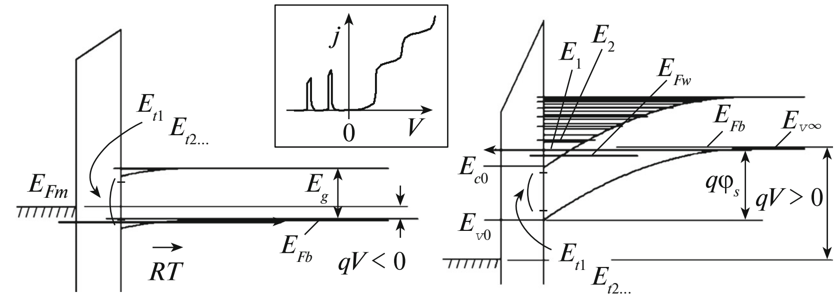

Fig. 1. Band diagrams of the Al/SiO$_2$/p^+-Si RTD at the voltage of activation of the subband E_1 (on the right) and at the voltage of activation of one of the SS. The position of Fermi level E_{Fw} of the quantum well is determined by the balance of currents of electron arrival to the QW and electron escape from the QW. Schematic of the j–V characteristic of the RTD (between the band diagrams).

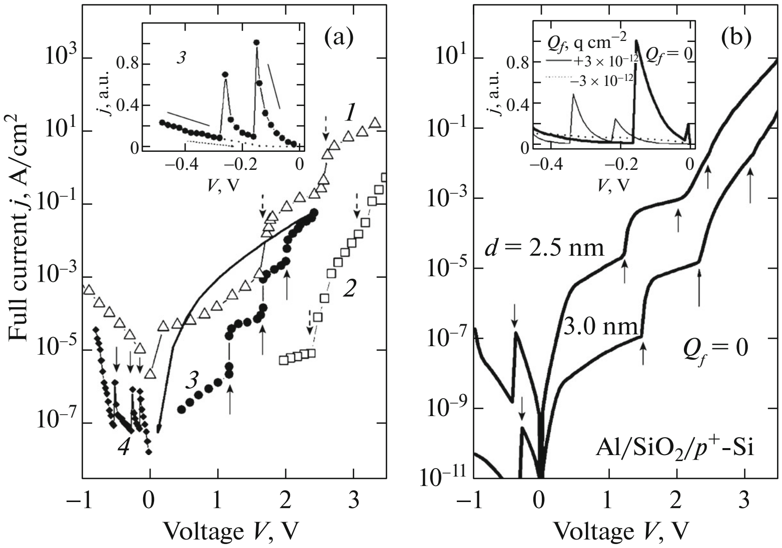

Fig. 2. (a) Experimental and (b) calculated j–V characteristics of the Al/SiO$_2$/p^+-Si (10^{19} cm^{-3}) RTD with nonlinearities in the form of current steps and peaks. (*1*, *2*) RTDs with thermal oxide and (*3*, *4*) RTDs with electrochemical oxide. For sample *3*, hysteresis is observed. RT activation voltages are shown by vertical arrows. Inset: (a) variation in the number of peaks vs. the voltage variation program and (b) effect of the charge in the oxide (d = 3 nm) on the number of current peaks.

dictated by the relation between Fermi energies $E_{Fb|m}$ of bulk silicon and metal (Fig. 1). At $E_{Fb} > E_{Fm}$ ($V > 0$), both the emitter and collector have a large energy width and the activation of the level is reflected by a current step in the j–V characteristic. At $E_{Fb} < E_{Fm}$ ($V < 0$), electrons are collected in the narrow strip of free states below the v-band edge $E_{v\infty}$ of bulk Si, which leads to an occurrence of peaks in the j–V characteristic. The RT nonlinearities are schematically shown in Fig. 1.

The described features in the behavior of the MIS structures were observed in experiments. Figure 2a shows j–V characteristics for several Al/SiO$_2$/p^+-Si samples ($N_A \sim 10^{19}$ cm^{-3}, and flat band voltage is $V_{FB} \sim -1$ V). The SiO$_2$ layer ($d \sim 2$–4 nm) was formed by dry thermal oxidation at 700°C for 30 min for sample *1* and 40 min for sample *2* or by electrochemical oxidation at 20°C for samples *3* and *4*. The behavior of the structures at $V > 0$ was qualitatively independent of a chosen technique, but the peaks in the range of $V_{FB} < V < 0$ are more typical for the electrochemical oxide. The voltage of the first current rise at $V > 0$ varied from 1.0 to 2.5 V; as dielectric thickness d was increased, the rise shifted to the right. We managed to obtain two to three steps and three to five peaks.

In the samples with the electrochemical oxide, it was noticed that the number of peaks at $V < 0$ can increase if the system was involved in the RT at $V > 0$. One more feature is the hysteresis of the j–V characteristic typical of structures with relatively thick (≥3–4 nm) SiO$_2$ and not with thinner insulators. An example is sample *3* (Fig. 2a, the recording rate is ~1 V/min). After passing three steps at $V > 0$, the $j(V)$ curve is placed higher for decreasing voltage and at $V < 0$ passes to the j–V characteristic with peaks with increasing $|V|$ (see inset in Fig. 2a), which are not repeated upon recovered to zero, but returned after the RT at $V > 0$.

We simulated the RT of electrons in the MIS RTD. Since the algorithms for calculating the characteristics of MIS structures was described by us previously [6], we only consider the calculation of two RT currents of different nature: j_w^{RT} through the QW levels and j_t^{RT} through the SS levels. Electron concentrations N_i at levels E_i of the QW are distributed in accordance with the Fermi function $f_w(E, E_{Fw})$. These concentrations and Fermi energy E_{Fw} are determined from the condition of balance of the resulting currents of electron arrival and escape over all the QW levels

$$\begin{aligned} J_w^{RT} &= \frac{q}{\pi\hbar^2}\sum_{E_i}\frac{\zeta_i m_i}{\tau_{ar,i}}\int (f_w - f_m)T_{ox}dE \\ &= \frac{q}{\pi\hbar^2}\sum_{E_i<q\varphi_s-E_g}\frac{\zeta_i m_i}{\tau_{ar,i}}\int (f_b - f_w)T_s dE, \end{aligned} \tag{1}$$

and

$$N_i = \frac{\zeta_i m_i k_B t}{\pi\hbar^2}\ln\left[1+\exp\frac{E_{Fw}-E_i}{k_B t}\right]. \tag{2}$$

Here, $T_{ox|s} = T_{ox|s}(E, E_\perp)$ is the probability of tunneling of the electron with a total energy E and a transverse energy $E_\perp = E - E_i$ through the oxide (ox) or silicon (s) barriers; $f_{b|w|m}(E, E_{Fb|w|m})$ is the Fermi function in the bulk of p^+-Si (b), QW (w), and metal (m); $\tau_{ar,\,i}$ is the time of passage of the QW by the electron back and forward; m_i and ζ_i are the effective mass and degeneracy for levels E_i ($i = 1, 2, \ldots$); and t is the temperature (300 K). Concerning the SS, their occupancies by electrons v_{t1}, v_{t2}, ..., in contrast to the case of the QW, are determined from the condition of balance between electron arrival and escape for each separate state. We obtain

$$v_{ti} = (T_{ox} f_m + T_s f_b)(T_{ox} + T_s)^{-1}, \tag{3}$$

and

$$\begin{gathered} j_{ti}^{RT} = qN_{ti}T_{ox}T_s\tau_t^{-1}(f_b - f_m)(T_{ox} + T_s)^{-1}, \\ J_t^{RT} = \sum j_{ti}^{RT}. \end{gathered} \tag{4}$$

Probabilities $T_{ox|s}$ in (3) and (4) are calculated with $E_\perp = 0$ and total energy equal to SS energy E_{ti}. Here, N_{t1}, N_{t2}, ... are the densities of the SS and τ_t is the lifetime in them. Taking into account that the SS are an acceptor in the upper half of the band gap and donor in its lower part [5], the total charge ($\mathrm{C \cdot cm^{-2}}$) on the Si/SiO$_2$ interface is

$$\begin{aligned} Q_s = -qN_s = q\Bigg[&-\sum_{i=1,2,\ldots} N_i \\ &- \sum_{E_{ti} > -E_g/2} v_{ti}N_{ti} + \sum_{E_{ti} < -E_g/2} (1 - v_{ti})N_{ti} \Bigg]. \end{aligned} \tag{5}$$

A contribution to the field $F_{\mathrm{SiO_2}}$ in SiO$_2$ is made, along with Q_s, by the charge of the depleted silicon region with width w ($Q_{depl} = -qwN_A$) and, possibly, by relatively slow mobile charge Q_f in the oxide near the interface with Si. In the MIS RTD, along with the RT current, there is a current c band–metal, which is limited by the low rate of thermal generation and, consequently, low current j_d of electron drift in the c band [3, 6]. This current maintains the regime necessary for the RT. In addition, there is the excess tunnel current v band–metal.

The calculated j–V characteristics are shown in Fig. 2b. In the calculation of the SS, we made a standard assumption about the presence of levels E_{ti} slightly lower than E_{c0} and slightly higher than E_{v0}. For the sake of simplicity, we considered single SS levels with energies of –0.15 eV and $-E_g + 0.15$ eV, of density 10^{12} cm^{-2}, and $\tau_1 = 10^{-15}$ s; in the main plot, $Q_f = 0$. It can be seen (compare Figs. 2a and 2b) that the model reproduces the general shape of the j–V characteristic, i.e., the steps and one peak. The first current rise at $V > 0$ is caused by the RT activation via the acceptor SS; the second rise is caused by the RT activation via the QW level; the next rises at levels E_2, E_3, ... that are involved are more weakly pronounced. The peak is related to the RT via the donor SS; if we consider several such states, the number of peaks can grow (inset in Fig. 2b). Concerning the current values in Fig. 2b, there is no rough discrepancy with the measurement data, but a full quantitative comparison is still complicated by the inhomogeneous thickness of the SiO$_2$ film.

It is fundamentally important to take into account the existence of the nonzero SS density, although sometimes the model without SS describes fairly well the behavior of structures with thermal oxide—in particular, the voltage of the first current rise. However, the first rise often appears earlier, especially for samples with electrochemical SiO$_2$, and the second rise corresponds to the calculated activation of the QW level. Then, the participation of the SS allows the first step to be reproduced. The role of the SS appears even more important under negative biases: to obtain at least one $j(V)$ peak without the SS, it would be necessary to introduce an unreal large Q_f value. At the same time, assuming that the peaks can be caused by the SS, the density of the latter should not be anomalously high.

The variable number of peaks observed at $V < 0$ (inset in Fig. 2a) may be due to variation in charge Q_f in SiO$_2$. When a positive voltage is applied to the metal, the SiO$_2$/Si interface attracts positively charged radicals or ions from the oxide, which move off this interface at $V < 0$ or are even replaced by negative ions. The calculation shows (inset in Fig. 2b) that the moderate Q_f variations can change the number of features left-of-zero. The hysteresis of the j–V characteristic at $V > 0$ (Fig. 2a) is probably related to the appearance of a significant negative charge in the well or on the acceptor levels. When the RT stops with decreasing voltage, occupation of the levels by electrons continues for some time, which leads to the current hysteresis noticeable even at a sweep rate of ~1 V/min. The charge leakage occurs via the tunnel resistance of the oxide and substrate capacitance; estimations with regard to possible values confirm the reality of this process.

To fully understand the conditions for electron storage (certainly, we are more interested in the storage in the QW than on the SS), we calculated some MIS RTD parameters as functions of oxide thickness d. Figure 3 shows the thickness dependences of the mutual position of the Fermi quasi-levels in the bulk of Si and in the well ($E_{Fb} - E_{Fw}$), resulting electron concentration ΣN_i on the QW levels, total current j, and probability ratio $T_s/T_{ox} = T_s(E_1, 0)/T_{ox}(E_1, 0)$. A regime similar to that for the RT is specified by fixing the field in SiO$_2$ ($F_{\mathrm{SiO_2}} = 6.8 \times 10^6$ V/cm), so one subband (E_1) is involved in the RT over the entire d range. It can be seen that, as the SiO$_2$ thickness is increased, energy E_{Fw} approaches E_{Fb}. The electron concentration in the QW simultaneously grows and attains ~10^{12} cm^{-2}, which is quite sufficient to affect the current dynamics. The required excess of the tunnel transparency of the semiconductor barrier over the

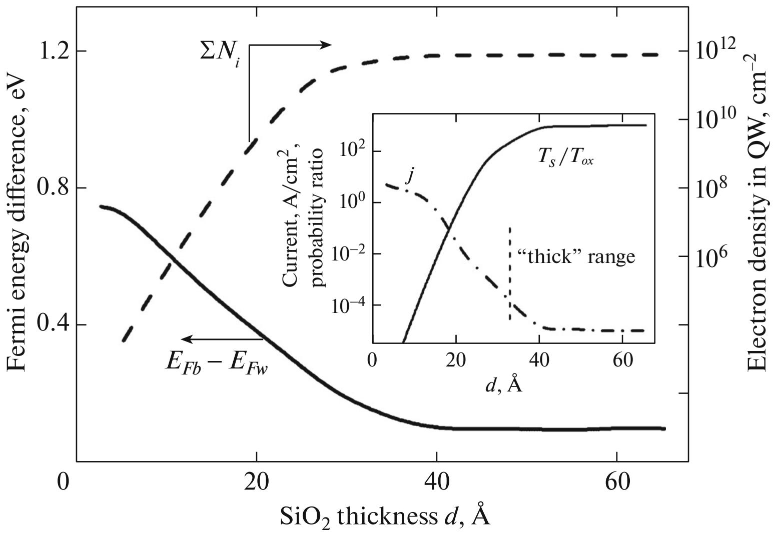

Fig. 3. Calculated electron concentrations in the Al/SiO$_2$/p^+-Si (10^{19} cm^{-3}) RTD QW and difference between the Fermi energies of bulk Si and QW vs. oxide thickness. Inset: variation in the total current and ratio of the tunnel transparencies of the barriers with the SiO$_2$ thickness.

transparency of the oxide barrier ($T_{ox} \ll T_s$) is implemented in the thick oxide limit. Note that, under the chosen conditions of the fairly strong field $F_{\mathrm{SiO_2}}$ = const, in contrast to V = const, the role of drift current j_d as a factor of well filling remains insignificant with increasing d.

To conclude, we would like to emphasize the two results obtained. First, we demonstrated the operation of the MIS structure as an RTD and the importance of taking into account the transit role of the SS in resonant tunneling. Second, we showed the possibility of attaining high electron concentrations in the QW of the MIS RTD.

The investigated RTD differs from traditional resonant-tunneling diodes [7] in its simpler design and the combination of materials of silicon integral electronics wherein it can be employed.

REFERENCES

1. J. Robertson and R. W. Wallace, Mater. Sci. Eng. R **88**, 1 (2015).
2. R. C. Ranuárez, M. J. Deen, and C. H. Chen, Microelectron. Reliab. **46**, 1939 (2006).
3. G. G. Kareva and M. I. Vexler, Fiz. Tekh. Poluprovodn. **47**, 1087 (2013).
4. G. G. Kareva, M. I. Vexler, and Yu. Yu. Illarionov, Microelectron. Eng. **109**, 270 (2013).
5. V. A. Gurtov, *Solid State Electronics* (Tekhnosfera, Moscow, 2008) [in Russian].
6. M. I. Vexler, S. E. Tyaginov, Yu. Yu. Illarionov, Yew Kwang Sing, Ang Diing Shenp, V. V. Fedorov, and D. V. Isakov, Semiconductors **47**, 686 (2013).
7. J. P. Sun, G. I. Haddad, P. Mazumder, and J. N. Schulman, Proc. IEEE **86**, 641 (1998).

Translated by E. Bondareva